THE JOURNAL OF BIOLOGICAL CHEMISTRY VOL. 286, NO. 45, pp. 39573–39584, November 11, 2011

Endoplasmic Reticulum Localization of DHHC Palmitoyltransferases Mediated by Lysine-based Sorting Signals*

Received for publication, June 15, 2011, and in revised form, September 15, 2011 Published, JBC Papers in Press, September 18, 2011, DOI 10.1074/jbc.M111.272369

Oforiwa A. Gorleku[‡], Anna-Marie Barns[‡], Gerald R. Prescott[§], Jennifer Greaves[‡], and Luke H. Chamberlain[‡1]

From the [‡]Strathclyde Institute of Pharmacy and Biomedical Sciences, University of Strathclyde, 161 Cathedral Street, Glasgow G4 0RE, United Kingdom and the [§]School of Biology, Medical and Biological Sciences Building, University of St. Andrews, North Haugh, St. Andrews, Fife KY16 9TF, United Kingdom

Background: Mammalian genomes encode 24 "DHHC" *S*-palmitoyltransferases.
Results: Sorting signals were mapped in DHHC4/6, and the localization of DHHC3 was shown not to impact substrate palmitoylation.
Conclusion: Lysine-based signals target DHHC4/6 to the endoplasmic reticulum, and DHHC3 localization is a primary determinant of site of substrate palmitoylation.
Significance: This work highlights how DHHC protein targeting is regulated and the relationship between DHHC targeting and substrate palmitoylation.

Intracellular palmitoylation dynamics are regulated by a family of 24 DHHC (aspartate-histidine-histidine-cysteine) palmitoyltransferases, which are localized in a compartment-specific manner. The majority of DHHC proteins localize to endoplasmic reticulum (ER) and Golgi membranes, and a small number target to post-Golgi membranes. To date, there are no reports of the fine mapping of sorting signals in mammalian DHHC proteins; thus, it is unclear how spatial distribution of the DHHC family is achieved. Here, we have identified and characterized lysine-based sorting signals that determine the restricted localization of DHHC4 and DHHC6 to ER membranes. The ER targeting signal in DHHC6 conforms to a KK*XX* motif, whereas the signal in DHHC4 is a distinct K*XX* motif. The identified dilysine signals are sufficient to specify ER localization as adding the C-terminal pentapeptide sequences from DHHC4 or DHHC6, which contain these K*XX* and KK*XX* motifs, to the C terminus of DHHC3, redistributes this palmitoyltransferase from Golgi to ER membranes. Recent work proposed that palmitoylation of newly synthesized peripheral membrane proteins occurs predominantly at the Golgi. Indeed, previous analyses of the peripheral membrane proteins, SNAP25 and cysteine string protein, are fully consistent with their initial palmitoylation being mediated by Golgi-localized DHHC proteins. Interestingly, ER-localized DHHC3 is able to palmitoylate SNAP25 and cysteine string protein to a similar level as wild-type Golgi-localized DHHC3 in co-expression studies. These results suggest that targeting of intrinsically active DHHC proteins to defined membrane compartments is an important factor contributing to spatially restricted patterns of substrate palmitoylation.

S-Palmitoylation has emerged over recent years as a highly versatile regulator of diverse cellular proteins. Prominent roles for palmitoylation include regulating protein-membrane interactions, protein targeting to defined intracellular membranes or membrane subdomains, and protein stability (1–4). A major breakthrough in the palmitoylation field came through studies in yeast that identified palmitoyltransferases that were active against Ras and casein kinase (5, 6); comparison of the amino acid sequences of these palmitoyltransferases, Erf2 and Akr1, revealed a common 51-amino acid "DHHC"-cysteine-rich domain that was essential for palmitoylating activity. These studies were pivotal in defining palmitoylation as an enzymatic process and led to the subsequent identification of DHHC palmitoyltransferases in higher organisms; in mammals, at least 24 DHHC proteins are genetically encoded (7, 8).

The recent development of techniques that allow purification of bulk cellular palmitoylated proteins combined with proteomic approaches has led to the description of palmitoylomes from several cell types (9–11). These studies have captured the diversity of palmitoylated substrates and highlighted palmitoylation as a prominent post-translational modification. In the rodent brain, more than 250 proteins are palmitoylated (10), which can be broadly classified as peripheral or integral membrane proteins. Peripheral proteins, such as Ras, Gα subunits, and Src family kinases, are dependent upon palmitoylation for membrane association (4).

Palmitoylation is a highly dynamic process, and many soluble proteins undergo continuous cycles of palmitoylation and depalmitoylation (4). Seminal work suggested a model to explain how this dynamic palmitoylation acts to control the precise intracellular distribution of mammalian Ras proteins as follows (12, 13): following synthesis, H- and N-Ras are farnesylated on a C-terminal CAA*X* motif, providing a weak membrane affinity that allows transient interaction with any intracellular membrane; when transiently associating with the Golgi, farnesylated Ras is recognized by Golgi-localized DHHC

* This work was supported by a senior non-clinical fellowship award from the United Kingdom Medical Research Council (to L. H. C.).
[1] To whom correspondence should be addressed. Tel./Fax: 44-141-548-3719; E-mail: Luke.Chamberlain@strath.ac.uk.

protein(s), resulting in palmitoylation and stable membrane attachment; membrane anchoring of Ras at the Golgi facilitates forward trafficking to the plasma membrane; and depalmitoylation on any membrane compartment releases Ras back into the cytosol, and the cycle of transient membrane interaction/palmitoylation continues.

A subsequent study that monitored temporal changes in the intracellular distribution of microinjected farnesylated N-Ras suggested that Ras palmitoylation is spatially restricted to the Golgi (14). Furthermore, all of the other peripheral membrane proteins that were examined in this study were also suggested to be palmitoylated at the Golgi following their biosynthesis, consistent with the notion that this membrane compartment acts as a superreaction center for the palmitoylation of newly synthesized soluble proteins (14). However, it is important to note that this study did not directly monitor palmitoylation, and indeed previous work has shown that Erf2, the DHHC protein that palmitoylates yeast Ras, is localized to the ER[2] (15). Furthermore, a very limited set of palmitoylation substrates was examined in this study. Thus, additional work is clearly required to more rigorously test the hypothesis that the Golgi is the predominant site for palmitoylation of peripheral membrane proteins. Nevertheless, it should be noted that the idea that palmitoylation of peripheral membrane proteins occurs predominantly at the Golgi in mammalian cells is consistent with other studies that have highlighted Golgi-localized DHHC proteins as being active against a range of peripheral proteins in co-expression studies (16–19).

If the Golgi is a specialized reaction platform for the palmitoylation of peripheral proteins, how might this be achieved? Possibilities include the following: (i) DHHC proteins active against peripheral membrane proteins are restricted to the Golgi to ensure spatial control of palmitoylation of this class of proteins; (ii) association of DHHC proteins with membrane compartments, such as the endoplasmic reticulum, is incompatible with palmitoyltransferase function; and (iii) co-factors required for efficient palmitoylation are present only at the Golgi.

At present, there is very little information available on how the spatial distribution of the cellular palmitoylation machinery is achieved and the correlation between DHHC substrate specificity and substrate intracellular localization. The aims of the present study were 2-fold: to identify signals that mediate targeting of DHHC proteins to a defined intracellular location (in this case the ER) and to use this information to test the hypothesis that DHHC activity toward peripheral proteins is restrained by compartmental specificity.

EXPERIMENTAL PROCEDURES

Plasmids—SNAP25 and cysteine-string protein (CSP) constructs with N-terminal EGFP tags were as described previously (20, 21). HA-tagged versions of DHHC3, DHHC4, and DHHC6 were kindly provided by Dr. Masaki Fukata (National Institute of Physiological Sciences, Osaka, Japan) (7). Mcherry-Rab11 was as described previously (22). TGN38-GFP was a gift from Professor George Banting (University of Bristol) (23). Untagged DHHC4 was generated by inserting the coding sequence and stop codon of this protein into the pEGFP-N1 (Clontech) vector backbone between HindIII and SalI sites. All other mutant constructs used in this study were generated by site-directed mutagenesis and verified by DNA sequencing (University of Dundee DNA Sequencing Service).

Antibodies—A rabbit polyclonal GM130 antibody was obtained from Abcam (Cambridge, UK), mouse monoclonal HA antibody used for cell staining was from Cambridge Bioscience (Cambridge, UK), rat antibody against HA used for immunoblotting was from Roche Applied Science (East Sussex, UK), and mouse monoclonal GFP antibody (JL8) was from Clontech. DHHC4 antibody was purchased from Sigma.

Cell Culture and Transfection—PC12 cells were cultured in RPMI1640 containing 10% horse serum and 5% fetal calf serum at 37 °C in a humidified atmosphere containing 7.5% CO_2. For immunofluorescence analyses, PC12 cells were plated onto poly-D-lysine-coated glass coverslips and transfected with 0.5 μg of each plasmid using Lipofectamine 2000 (Invitrogen). Approximately 40 h post-transfection, the cells were fixed and stained with antibodies prior to confocal microscopy analysis.

HEK293 and HEK293T cells were maintained in DMEM supplemented with 10% fetal calf serum at 37 °C in a humidified atmosphere containing 5% CO_2. Cells were plated onto 24-well plates and analyzed ~20 h post-transfection.

Cell Fixation and Labeling—Transfected cells on coverslips were washed in PBS and fixed in 4% formaldehyde for 30 min at room temperature. The cells were then washed in PBS containing 0.3% BSA (PBSB) and permeabilized in PBSB containing 0.25% Triton X-100 for 6 min. The cells were washed and incubated with primary antibodies (1:50) in PBSB for 1 h and then with the appropriate Alexa Fluor-conjugated secondary antibodies (1:400) for 1 h. The specific antibodies that were used for each experiment are indicated in the figure legends.

Confocal Microscopy and Image Analysis—Image data were acquired on a Leica SP5 confocal microscope at Nyquist sampling rates and deconvolved using Huygens software (Scientific Volume Imaging). ImageJ software was used to calculate Pearson's correlation coefficient (R) values for co-variance of the fluorescence signals. Images shown that were not analyzed quantitatively were not processed by deconvolution.

Analysis of Palmitoylation by [^{3}H]Palmitate Labeling—For analysis of DHHC palmitoylation, HEK293T cells were transfected with 1 μg of the respective plasmids. For analysis of CSP or SNAP25 palmitoylation, cells were transfected with EGFP-tagged SNAP25/CSP (0.8 μg) and HA-DHHC (1.6 μg) constructs. Approximately 20 h post-transfection, the cells were incubated in [^{3}H]palmitic acid (0.5 mCi/ml) in DMEM with 1% defatted BSA for 3 h at 37 °C. The cells were washed and lysed in SDS dissociation buffer. The samples were resolved by SDS-PAGE and transferred to nitrocellulose membranes for immunoblotting analysis or exposed to film with the aid of a Kodak Biomax Transcreen LE intensifier screen for detection of [^{3}H]palmitate incorporation.

Analysis of CSP Palmitoylation by Band Shift—HEK293 cells were transfected with EGFP-CSP (0.8 μg) and HA-DHHC (1.6

[2] The abbreviations used are: ER, endoplasmic reticulum; CSP, cysteine string protein; TGN, *trans*-Golgi network; ANOVA, analysis of variance; BFA, brefeldin A.

μg) constructs. Approximately 20 h post-transfection, the cells were washed and lysed in SDS dissociation buffer. The samples were resolved by SDS-PAGE and transferred to nitrocellulose membranes for immunoblotting analysis.

RESULTS

The C-terminal Pentapeptide Sequences in DHHC4 and DHHC6 Are Required for ER Localization—Previous studies have identified dilysine-based ER localization motifs located at the extreme C termini of specific proteins, which conformed to the sequence K*X*K*XX* or KK*XX* (with the final *X* representing the terminal residue in a protein sequence) (24) (Fig. 1*A*). Very little information is currently available to describe how DHHC protein targeting is regulated. Thus, we screened the sequences of the 24 mammalian DHHC proteins to assess whether any of these proteins contain possible ER localization signals conforming to these consensus motifs.

DHHC4 and DHHC6 both contain possible dilysine-based ER targeting signals at their C termini (Fig. 1*A*). Furthermore, both of these proteins localized to the ER, displaying marked overlap in fluorescence profiles with RFP-ER (which consists of the KDEL ER retrieval motif fused to red fluorescent protein) (Fig. 1*B*). Interestingly, when the C-terminal 5 amino acids were removed from DHHC4 and DHHC6, the proteins lost their restricted distribution at the ER (Fig. 1*B*). The DHHC4(1–338) mutant was redistributed to the Golgi, displaying a marked overlap with GM130 (Fig. 1*C*), whereas DHHC6(1–408) associated with the plasma membrane and an intracellular compartment that was proximal to but clearly distinct from the Golgi (Fig. 1*C*). Quantitative measurements of fluorescence intensity co-variance of the DHHC4/DHHC6 proteins *versus* RFP-ER and GM130 through whole cell image stacks were provided by calculating Pearson's correlation values (Fig. 1, *B* and *C*). This quantitative analysis confirmed a statistically significant decrease in co-variance of the DHHC4 and DHHC6 mutants with RFP-ER and an increase in co-variance with GM130 fluorescence signal. The level of change in the calculated *R* values going from two proteins with strong co-localization to two proteins with little co-localization is consistent with previous studies (25, 26).

It should be noted that an earlier publication reported that Myc-tagged DHHC4 localized to the Golgi in HEK293T cells (27), whereas a more recent study showed ER localization of the protein in primary neurons (28). Although DHHC4 was suggested to localize to the Golgi in HEK293T cells, no data were presented showing co-localization with Golgi marker proteins (27). Thus, we revisited DHHC4 localization in HEK293T cells to determine if DHHC4 exhibited a distinct localization in this cell type compared with PC12 cells. HA-tagged DHHC4 was clearly localized to the ER in HEK293T cells, showing strong overlap with RFP-ER (Fig. 2, *A* and *B*). Because it was formally possible that the HA tag on our construct might be perturbing normal DHHC4 targeting, we also constructed an untagged form of the protein, which was recognized by a commercial antibody (Fig. 2*C*). Untagged DHHC4 displayed an ER localization in both PC12 and HEK293T cells (Fig. 2*D*), confirming that the HA tag was not responsible for the ER localization of DHHC4. Note that the antibody used was not able to detect endogenous DHHC4, and thus we were unable to study the distribution of endogenously expressed DHHC4.

To more precisely define the ER targeting motif in DHHC6, single amino acid substitutions were introduced into the C-terminal pentapeptide, and fluorescence intensity co-variance against RFP-ER was quantified. Mutation of either Lys-410 or Lys-411 to alanine led to a marked and significant loss of fluorescence co-variance with RFP-ER, whereas the other mutations were without effect (Fig. 3). These results confirm that the ER localization signal in the C-terminal tail of murine DHHC6 conforms to the consensus KK*XX*. The sequence of the C-terminal pentapeptide in murine DHHC4 is KKKEK, which conforms to both K*X*K*XX* and KK*XX* consensus sequences. Thus, we examined the effects of individually mutating each lysine residue at the first, second, and third position of the KKKEK sequence. Surprisingly, only substitution of the third lysine (Lys-341) led to a loss of ER localization (Fig. 4); even when the first and second lysines were mutated in tandem, DHHC4 retained an ER distribution (Fig. 4). These findings suggest that the signals that regulate ER localization of DHHC4 are not completely conserved with DHHC6, and the ER targeting motif of DHHC4 conforms more to a K*XX* sequence. Indeed, bovine DHHC4 lacks a dilysine motif but does retain lysine 341 (see Fig. 1*A*).

ER Targeting Signals from DHHC4 and DHHC6 Are Sufficient to Relocate DHHC3 from Golgi to ER Membranes—Having identified ER targeting signals present within two distinct DHHC proteins, we next examined whether the C-terminal 5 amino acids from DHHC4 and DHHC6 (which contain the identified lysine-based sorting signals) were sufficient to relocate the Golgi-localized DHHC3 protein onto ER membranes. As a control, the sequence KGKRD (a *bona fide* signal sufficient for ER targeting from human UDP-glucuronyl transferase (24)) was also added to DHHC3. All three signals led to a loss of Golgi localization (co-variance with GM130; Fig. 5*A*) and a marked relocation to ER membranes marked by RFP-ER (Fig. 5*B*). Indeed, the movement of DHHC3 onto ER membranes was substantial, and we were unable to visually detect any overlap of the DHHC3 mutant proteins with GM130 staining (Fig. 5*A*). It was formally possible that the addition of these pentapeptides to DHHC3 led to ER retention by disrupting intrinsic Golgi targeting signals in the C terminus of DHHC3. However, this is unlikely to be the case because truncation of the C-terminal 50 amino acids from DHHC3 (DHHC3(1–250)) did not lead to ER retention (Fig. 5*B*).

ER-localized DHHC3 Proteins Are Palmitoylated and Retain Palmitoyltransferase Activity against Peripheral Proteins—Recent work by our group and others on the peripheral membrane proteins SNAP25 and CSP is consistent with the initial palmitoylation of these proteins taking place on Golgi membranes (16, 17, 21, 29). In addition, it has been suggested that the Golgi might be the focal point for palmitoylation of many peripheral membrane proteins (14). We have previously proposed that CSP and SNAP25 utilize an intrinsic weak membrane affinity of their cysteine-rich domains to "sample" intracellular membranes and seek out their partner DHHC proteins (16, 20, 21). The underlying reason for why palmitoylation of these proteins might be restricted to the Golgi is not clear, but this suggests

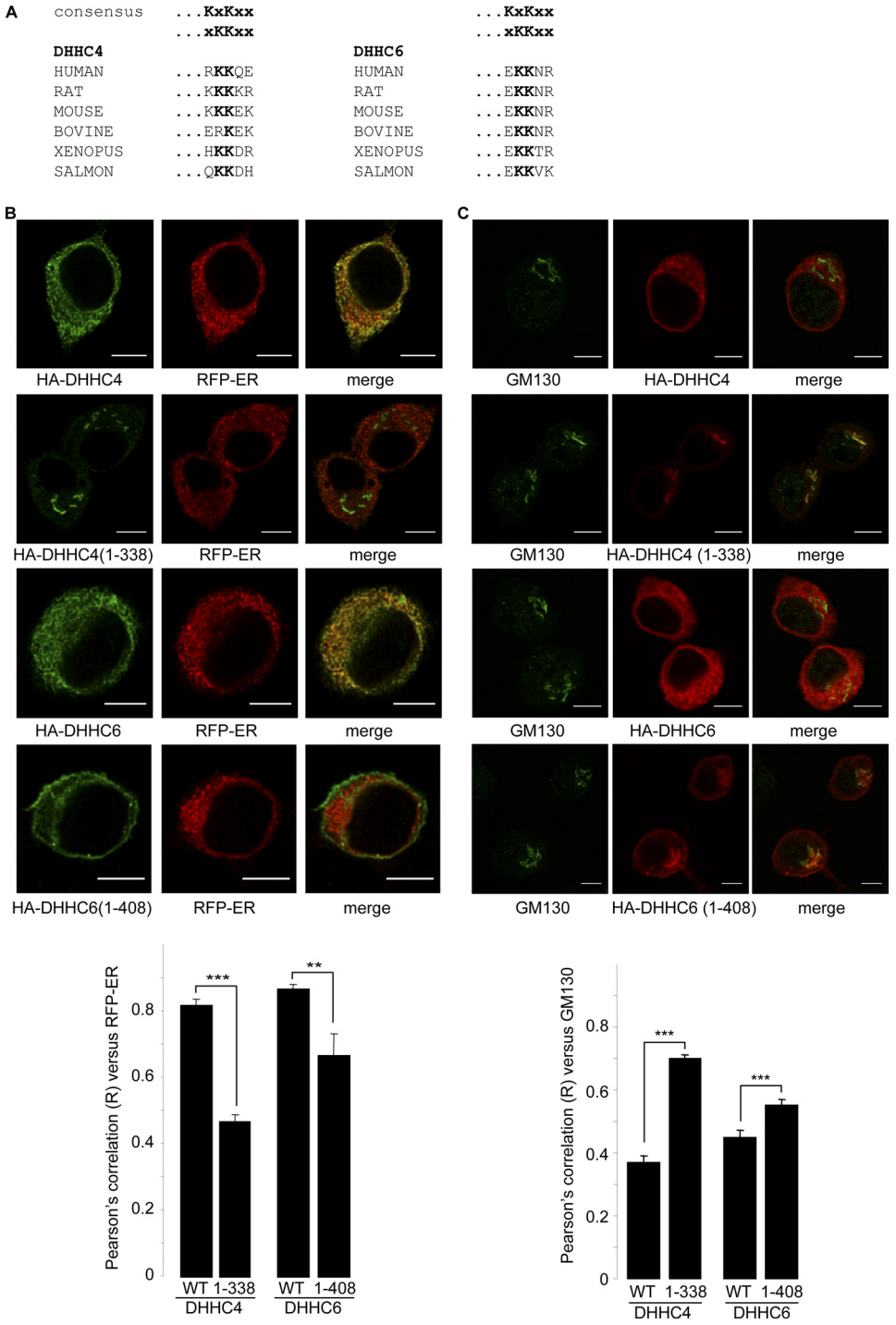

FIGURE 1. **C-terminal pentapeptide sequences are required for ER localization of DHHC4 and DHHC6.** *A*, the sequences of the final 5 amino acids in DHHC4 and DHHC6 proteins from various species are shown. The consensus sequences of recognized ER retrieval motifs are shown for comparison. *B*, full-length DHHC4/DHHC6 proteins or mutants lacking the final 5 amino acids (DHHC4(1–338) and DHHC6(1–408)) were co-transfected into PC12 cells with a plasmid encoding RFP-ER, which is sorted to the ER. The HA tag of the DHHC proteins was labeled with a mouse HA antibody and subsequently with anti-mouse Alexa Fluor 488. Representative images acquired using a Leica SP5 confocal microscope are shown. *Scale bars*, 5 μm. ImageJ software was used to determine the fluorescence intensity co-variance (Pearson's correlation co-efficient) of DHHC proteins against that of RFP-ER. The truncated forms of DHHC4 and DHHC6 both displayed a significant reduction in co-variance with RFP-ER compared with the full-length DHHC proteins when analyzed using Student's *t* test (**, $p < 0.01$; ***, $p < 0.001$; $n = 5–6$ cells for each protein). *C*, PC12 cells were transfected with plasmids encoding DHHC4, DHHC4(1–338), DHHC6, or DHHC6(1–408). The cells were labeled with mouse anti-HA and rabbit anti-GM130 and subsequently with anti-mouse antibody conjugated to Alexa Fluor 543 and anti-rabbit antibody conjugated to Alexa Fluor 488. Representative images acquired using a Leica SP5 confocal microscope are shown. *Scale bars*, 5 μm. The truncated forms of DHHC4 and DHHC6 both displayed a significant increase in co-variance with GM130 compared with the full-length DHHC proteins when analyzed using Student's *t* test (***, $p < 0.001$; $n = 5–8$ cells for each protein). *Error bars*, S.E.

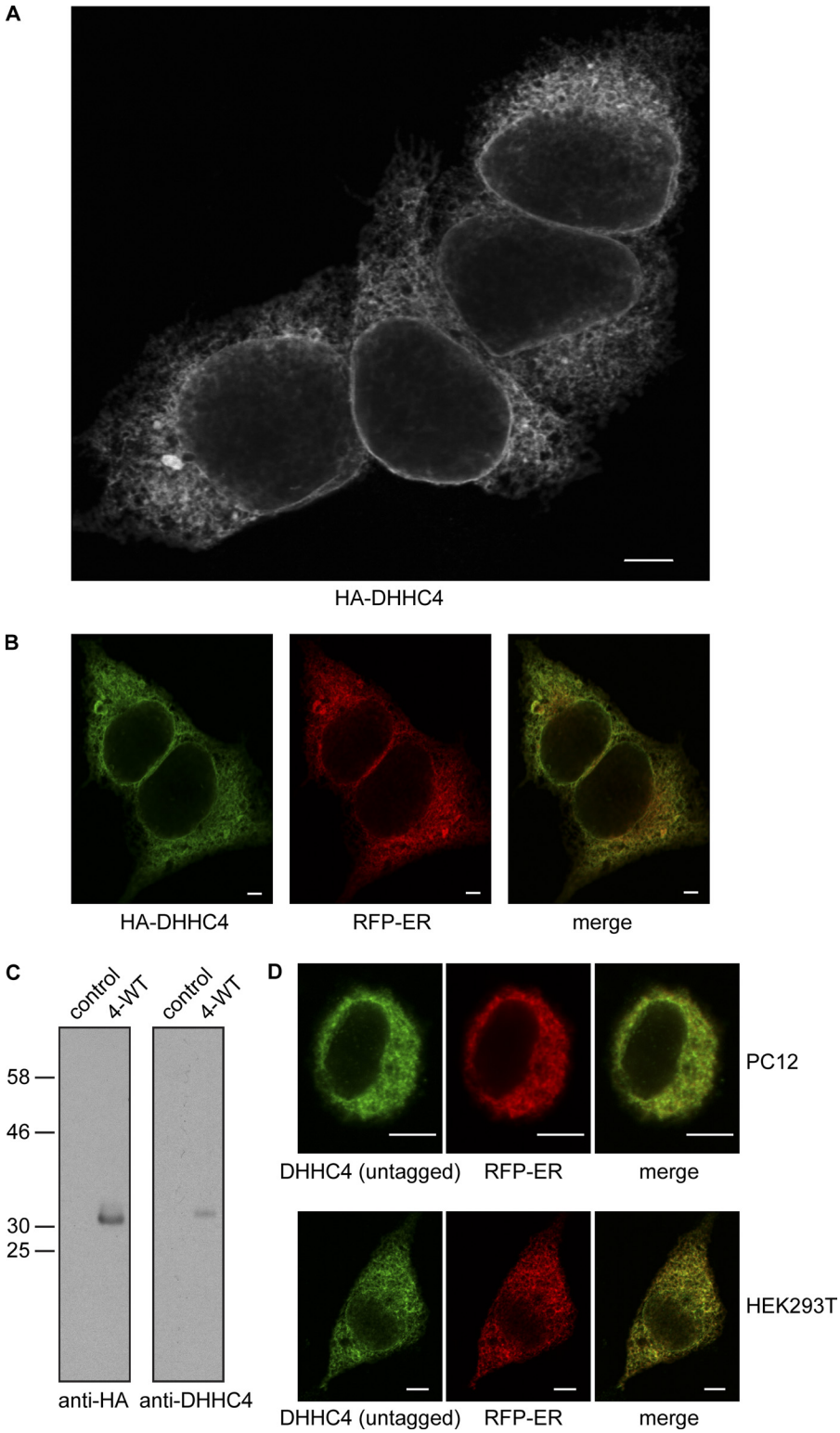

FIGURE 2. **Localization of HA-DHHC4 in HEK293T cells and untagged DHHC4 in PC12 and HEK293T cells.** *A*, a plasmid encoding HA-DHHC4 was transfected into HEK293T cells, which were labeled with anti-HA and subsequently with anti-mouse antibody conjugated to Alexa Fluor 488. A representative image acquired using a Leica SP5 confocal microscope is shown. *B*, as *A* except with co-transfection with a plasmid encoding RFP-ER. *C*, HEK293T cells were transfected with HA-DHHC4 (*4-WT*) or with empty vector (*control*). Lysates were resolved by SDS-PAGE and transferred to nitrocellulose for immunoblotting analysis using anti-HA or anti-DHHC4 antibodies. Positions of molecular weight markers are shown on the *left*. *D*, a plasmid encoding untagged DHHC4 was co-transfected with RFP-ER into PC12 cells (*top*) or HEK293T cells (*bottom*). The cells were subsequently labeled with anti-HA and then with anti-mouse antibody conjugated to Alexa Fluor 488. Representative images acquired using a Leica SP5 confocal microscope are shown. *Scale bars* in all *panels*, 5 μm.

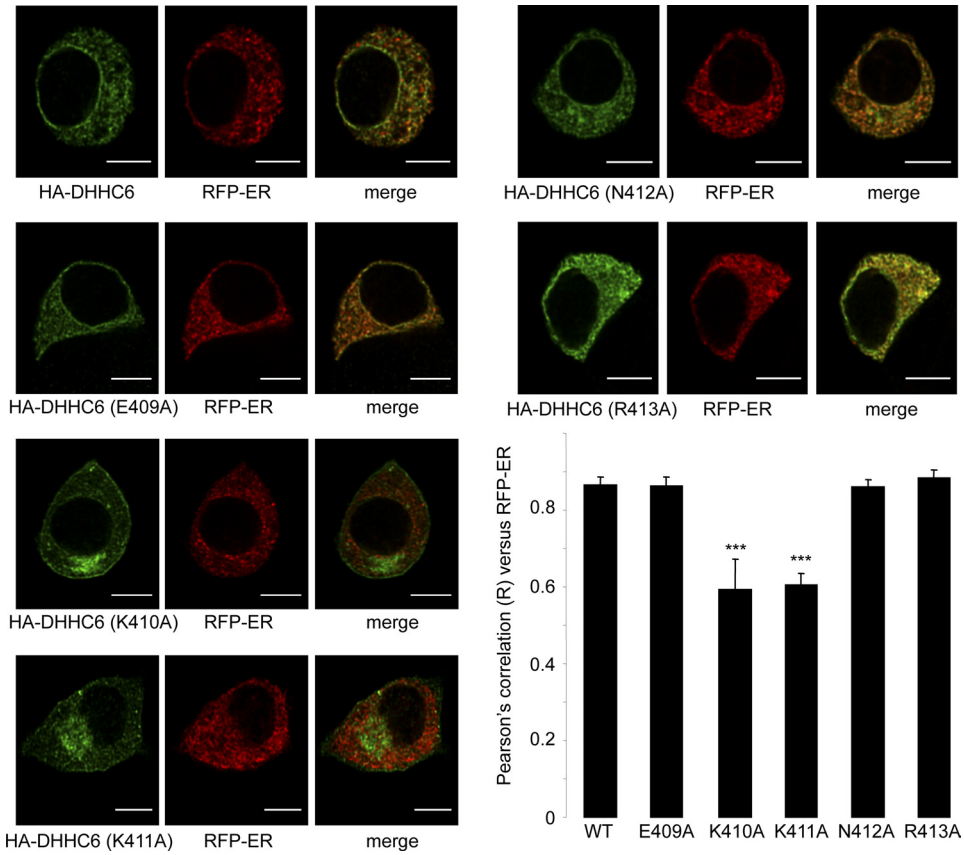

FIGURE 3. **Fine mapping of the ER localization motif in DHHC6.** Plasmids encoding DHHC6 with single point mutations in the C-terminal pentapeptide were co-transfected into PC12 cells with a plasmid encoding RFP-ER, which is sorted to the ER. The HA tag of the DHHC proteins was labeled with a mouse HA antibody and subsequently with anti-mouse antibody conjugated to Alexa Fluor 488. Representative images acquired using a Leica SP5 confocal microscope are shown. *Scale bars*, 5 μm. ImageJ software was used to determine the fluorescence intensity co-variance (Pearson's correlation co-efficient) of DHHC6 proteins against that of RFP-ER. The K410A and K411A DHHC6 mutants both displayed a significant decrease in co-variance with RFP-ER compared with wild-type DHHC6 when analyzed using a one-way ANOVA (***, $p < 0.001$; $n = 5$–7 cells for each protein). *Error bars*, S.E.

that there is a lack of DHHC activity against these proteins at the ER. We thus tested whether ER targeting of DHHC3 affects the activity of this protein. As a first step, we analyzed palmitoylation of wild-type DHHC3 in comparison with the ER-localized mutants. "Autopalmitoylation" of the DHHC domain is thought to be a prerequisite for subsequent palmitate transfer to substrate proteins. Because palmitoylation assays were performed in HEK293T cells, we first confirmed that wild-type DHHC3 and DHHC3 with an added dilysine motif display the same differential localization as was observed in PC12 cells (Fig. 6*A*). All of the ER-localized DHHC3 proteins displayed similar levels of palmitoylation as seen for wild-type DHHC3 in HEK293T cells (Fig. 6*B*). Interestingly, the ER-targeted DHHC3 proteins were observed to migrate at a faster rate than wild-type DHHC3 on SDS-polyacrylamide gels (Fig. 6*B*, *bottom*). This suggests that DHHC3 may undergo some post-translational modification following its exit from the ER.

We also examined the palmitoylation status of DHHC4 in comparison with DHHC3 and the Golgi-localized DHHC4-ΔKKKEK mutant. Fig. 6*B* shows that both wild-type and mutant DHHC4 are palmitoylated, albeit at lower levels than DHHC3 (Fig. 6*C*).

The finding that ER-localized forms of DHHC3 or DHHC4 are palmitoylated at levels similar to those of their Golgi counterparts provides evidence that the observed changes in localization of mutant proteins are not related to a loss of protein integrity (*i.e.* misfolding). Also, because palmitoylation of DHHC proteins is linked to their functional activity as palmitoyltransferases, this suggests that mutant forms of DHHC3/DHHC4 might retain similar activity as the wild-type proteins. Thus, we next examined if localization of DHHC3 to the ER affects its ability to palmitoylate specific substrate proteins. SNAP25b and CSP are palmitoylated by a subset of Golgi-localized DHHC proteins, including DHHC3, in co-expression studies (16, 17). Thus, EGFP-SNAP25b was co-transfected into HEK293T cells together with wild-type DHHC3 or the three ER-localized DHHC3 proteins, and the cells were labeled with [^{3}H]palmitic acid to monitor palmitoylation. Compared with control (co-transfection with empty vector), all DHHC3 proteins promoted a robust increase in [^{3}H]palmitate incorporation into SNAP25b (Fig. 7*A*). This suggests that DHHC3 proteins localized to the ER retain full palmitoyltransferase activity against this substrate protein. In addition to the Golgi, we have previously suggested that dynamic palmitoylation of mature SNAP25 might also occur at recycling endosomes and/or the *trans*-Golgi network (TGN) (17, 22). Thus, although we did not detect the dilysine mutants of DHHC3 at the Golgi by immunofluorescence (Fig. 5), it was formally possible that a small pool of these DHHC3 mutants might be associated with endosomes/TGN and that the observed palmitoylation of SNAP25

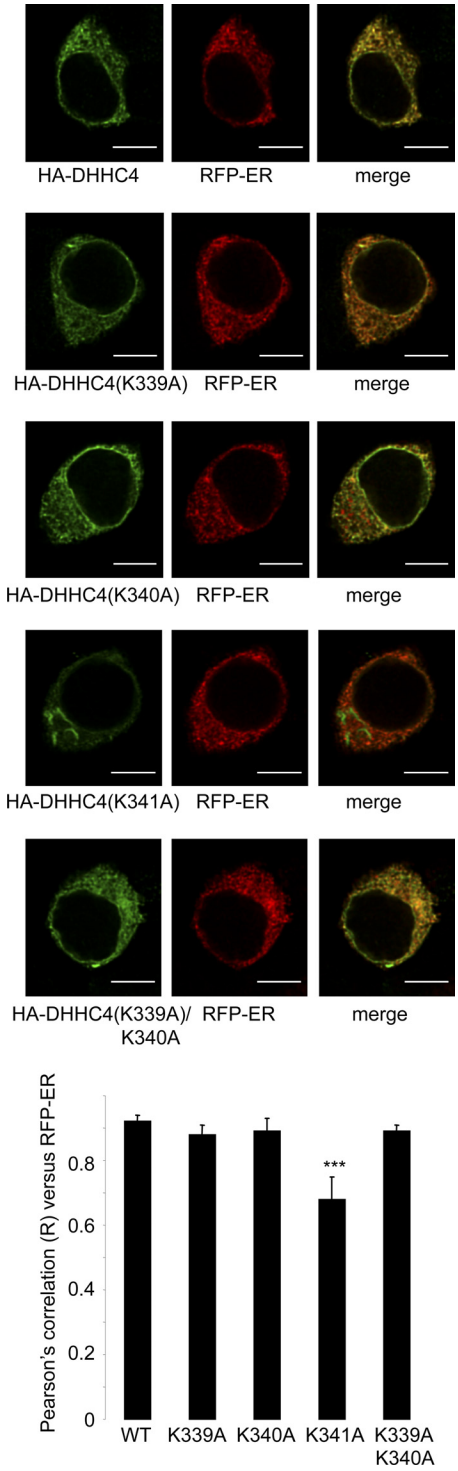

FIGURE 4. **Fine mapping of the ER localization motif in DHHC4.** Plasmids encoding DHHC4 with single point mutations in the C-terminal pentapeptide were co-transfected into PC12 cells with a plasmid encoding RFP-ER, which is sorted to the ER. The HA tag of the DHHC proteins was labeled with a mouse HA antibody and subsequently with anti-mouse Alexa Fluor 488. Representative images acquired using a Leica SP5 confocal microscope are shown. *Scale bars*, 5 μm. ImageJ software was used to determine the fluorescence intensity co-variance (Pearson's correlation co-efficient) of DHHC4 proteins against that of RFP-ER. The K341A DHHC4 mutant displayed a significant decrease in co-variance with RFP-ER compared with wild-type DHHC4 when analyzed using a one-way ANOVA (***, $p < 0.001$; $n = 4-6$ cells for each protein). *Error bars*, S.E.

might be occurring on these membrane compartments. Thus, we examined whether one of the mutants, DHHC3(KKKEK), displayed overlap with markers of recycling endosomes (Rab11) or TGN (TGN38) in PC12 cells. Fig. 7*B* shows that there was no noticeable overlap of DHHC3(KKKEK) with these membrane compartments, suggesting that the measured palmitoylation of SNAP25b reflected palmitoylation at the ER.

In addition to SNAP25, we also examined whether the ER-localized DHHC3 proteins were active against CSP. The palmitoylation of CSP can be easily monitored because it is accompanied by a marked hydroxylamine-sensitive band shift on SDS-polyacrylamide gels (Fig. 8*A*) (20). Fig. 8*B* demonstrates that co-expression of DHHC3 or one of the ER-localized DHHC3 proteins (in this case the KKKEK mutant) led to a marked increase in palmitoylation of CSP as revealed by a band shift on SDS gels. Furthermore, activity of all three ER-localized forms of DHHC3 toward CSP was confirmed by labeling with [^{3}H]palmitic acid (Fig. 8*C*). Both assays thus failed to uncover differences in palmitoylation of CSP by wild-type and ER-localized DHHC3.

Selective Palmitoylation of an ER-localized CSP Mutant by ER DHHC3 Mutants—We previously described a mutant form of CSP, in which 4 of the 14 palmitoylated cysteines are mutated to leucine residues (CSP(4CL)) (20). This mutant protein displays an increased membrane affinity and mislocalizes to ER membranes (20) (Fig. 9*A*). The CSP(4CL) mutant is not palmitoylated when expressed in cells, most likely due to a physical separation of the protein from its partner Golgi-localized DHHC proteins (20). Indeed, mixing of ER and Golgi membranes with BFA was previously shown to promote a robust palmitoylation of the 4CL mutant (16, 20). Because this CSP(4CL) protein is localized at the ER, we tested whether it would display differential palmitoylation by wild-type DHHC3 (Golgi-localized) and the ER-localized DHHC3 mutants. Indeed, in the absence of DHHC co-expression or with wild-type or inactive (DHHS) mutant DHHC3 co-expression, CSP(4CL) did not display a band shift on SDS gels that would be indicative of palmitoylation (Fig. 9*B*). Importantly, however, ER-localized DHHC3 mutants were able to palmitoylate the CSP(4CL) protein (Fig. 9*B*). This result provides strong evidence that DHHC3 is able to function as a palmitoyltransferase when localized to ER membranes.

DISCUSSION

The mammalian DHHC family was described in 2004 (7), but there is currently a lack of information on how intracellular patterning of these proteins is achieved or regulated. Targeting information for DHHC2 is contained within the C-terminal 68 amino acids, but the precise signals mediating intracellular targeting of this or other DHHC proteins have not been defined (30). Thus, the identification of ER localization signals in the C-terminal tails of DHHC4 and DHHC6 represents an important step toward delineating how DHHC proteins achieve their respective localizations.

Fine mapping of the ER localization signal in DHHC6 clearly showed that this conformed to the established consensus sequence KK*XX*. However, the results obtained with DHHC4 were more surprising. The sequence of the mouse DHHC4 ter-

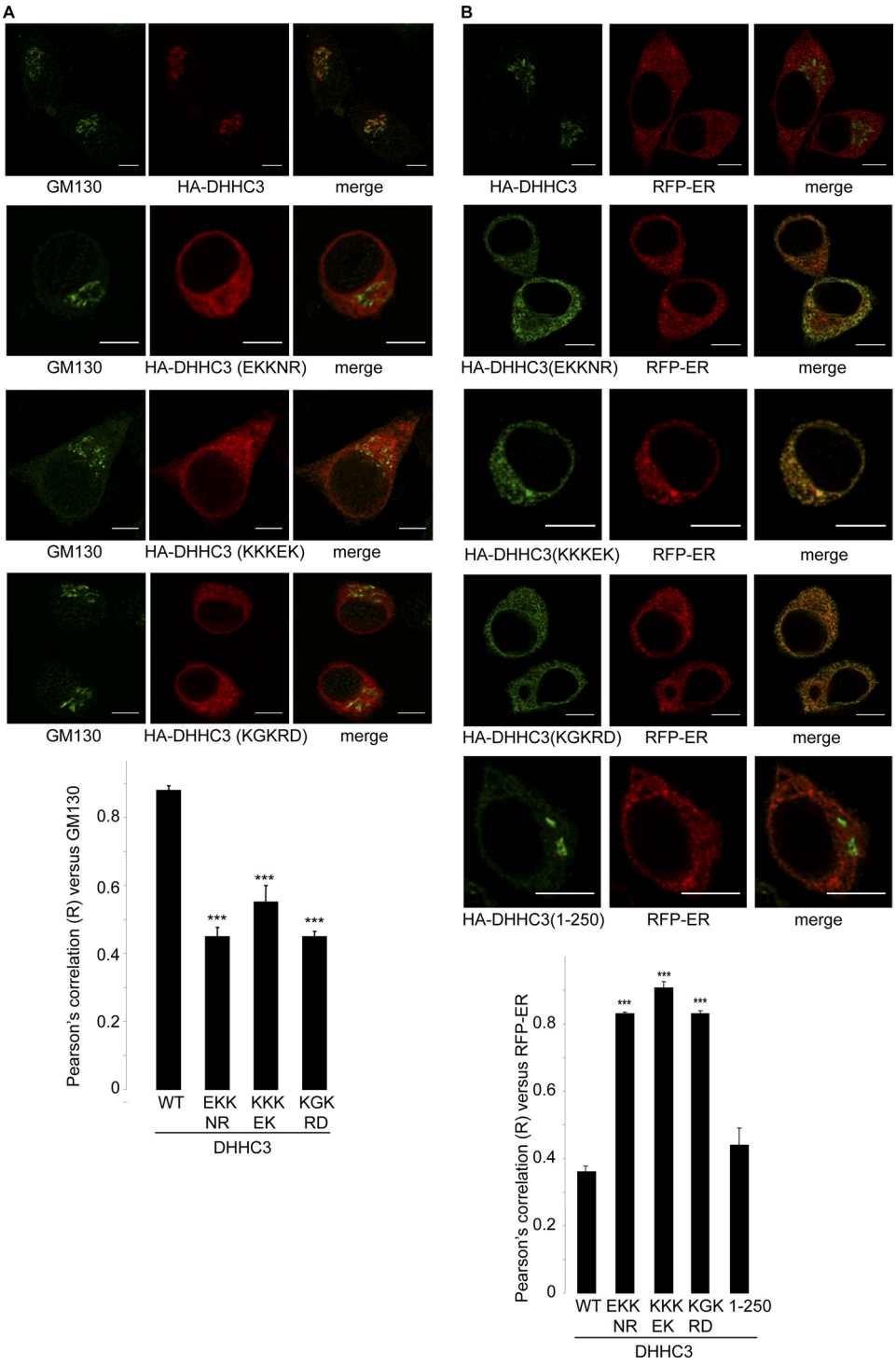

FIGURE 5. **C-terminal pentapeptides from DHHC4 and DHHC6 promote relocalization of DHHC3 onto ER membranes.** *A*, ER localization motifs from DHHC6 (EKKNR), DHHC4 (KKKEK), and UDP-glucuronyl transferase (KGKRD) were fused to the C terminus of DHHC3, and the constructs were transfected into PC12 cells. The cells were labeled with mouse anti-HA and rabbit anti-GM130 and subsequently with anti-mouse antibody conjugated to Alexa Fluor 543 and anti-rabbit antibody conjugated to Alexa Fluor 488. Representative images acquired using a Leica SP5 confocal microscope are shown. *Scale bars*, 5 μm. ImageJ software was used to determine the fluorescence intensity co-variance (Pearson's correlation co-efficient) of DHHC proteins against that of GM130. The DHHC3 mutants with ER localization motifs all displayed a significant reduction in co-variance with GM130 compared with wild-type (*WT*) DHHC3, assessed using a one-way ANOVA (***, $p < 0.001$; $n = 6–7$ cells for each protein). *B*, PC12 cells were co-transfected with DHHC3 plasmids and a plasmid encoding RFP-ER, which is sorted to the ER. The HA tag of the DHHC proteins was labeled with a mouse HA antibody and subsequently with anti-mouse antibody conjugated to Alexa Fluor 488. Representative images acquired using a Leica SP5 confocal microscope are shown. *Scale bars*, 5 μm. The DHHC3 mutant with ER localization motifs displayed a significant increase in co-variance with RFP-ER when analyzed using a one-way ANOVA (***, $p < 0.001$; $n = 5–7$ cells for each protein). A truncated DHHC3 protein lacking the C-terminal cytoplasmic domain (DHHC3(1–250)) did not show an increased level of co-variance with RFP-ER. *Error bars*, S.E.

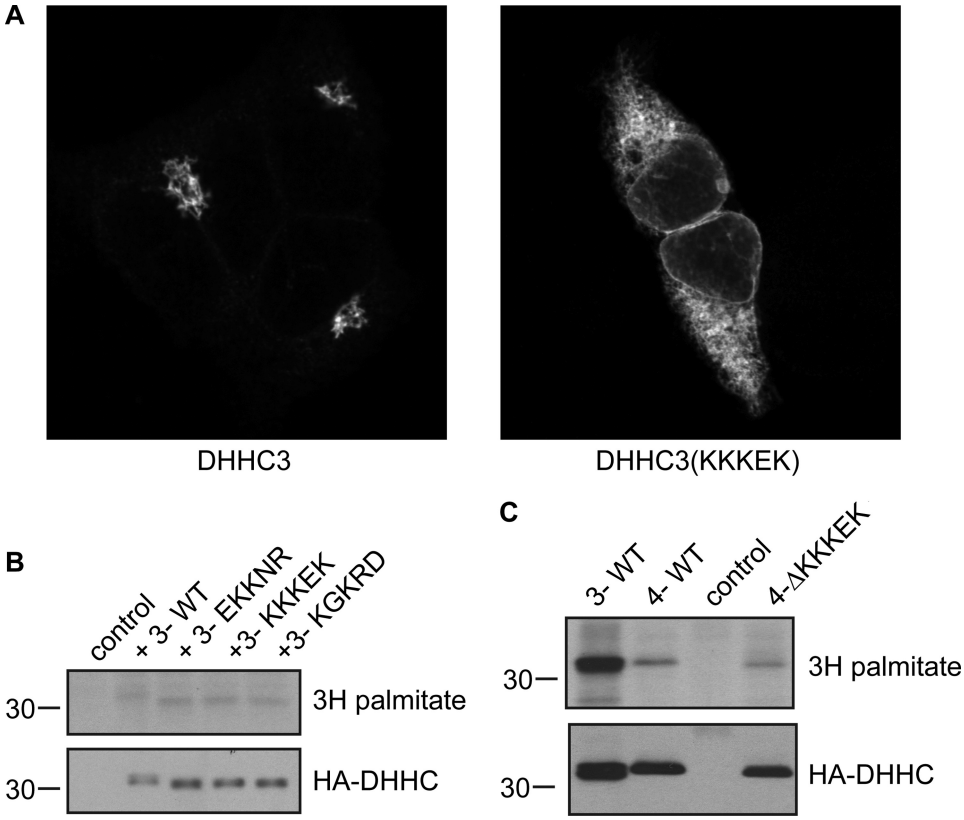

FIGURE 6. **Palmitoylation of wild-type and mutant DHHC proteins.** *A*, HEK293T cells were transfected with wild-type DHHC3 or DHHC3(KKKEK). The cells were fixed and stained with an anti-HA antibody and subsequently with anti-mouse antibody conjugated to Alexa Fluor 488. Representative images acquired using a Leica SP5 confocal microscope are shown. *B* and *C*, HEK293T cells were transfected with empty vector (control), wild-type DHHC3, or DHHC3 fused to the ER localization signals from DHHC6, DHHC4, or UDG-glucuronyl transferase (EKKNR, KKKEK, and KGKRD, respectively) (*B*) or with wild-type DHHC3, wild-type DHHC4, or DHHC4 lacking the C-terminal 5 amino acids (Δ*KKKEK*) (*C*). Twenty hours post-transfection, the cells were labeled with [^{3}H]palmitic acid for 3 h, lysed in sample buffer, resolved by SDS-PAGE, and transferred to duplicate nitrocellulose membranes. The membranes were exposed to film with the aid of a Kodak Biomax Transcreen LE intensifier screen for detection of [^{3}H]palmitate incorporation (*top panels*) or were probed with anti-HA for detection of expression levels of the DHHC proteins (*bottom panels*). The positions of molecular weight markers are shown on the *left* of all *panels*.

minal pentapeptide is KKKEK, conforming to both K*X*K*XX* and KK*XX* consensus motifs. However, we found that the lysines at positions 1 and 2 of the KKKEK sequence could be mutated in tandem without an effect on ER localization, whereas the third lysine (Lys-341) was essential for ER targeting. Interestingly a similar K*XX* sequence was identified as being important for ER localization of the membrane-bound progesterone receptor (31). Because a single lysine was not sufficient for ER localization of DHHC6, it is likely that other structural/sequence elements of DHHC4 contribute to ER targeting of this protein.

The identification of ER localization signals in DHHC4 and DHHC6 presented the opportunity to test how intracellular localization of DHHC family members affects their intrinsic palmitoylation activity. This issue is particularly relevant when one considers how spatially restricted palmitoylation might occur. The proteins studied here (SNAP25 and CSP) are modified by Golgi-localized DHHC proteins, and indeed the Golgi might be the primary site of palmitoylation of many such peripheral membrane proteins (14). Current evidence that palmitoylation of newly synthesized SNAP25 and CSP takes place at the Golgi includes the following observations: (i) palmitoylation and membrane binding of newly synthesized SNAP25 and CSP are only mediated by Golgi-localized DHHC proteins in co-expression studies (16, 17, 21); (ii) depletion of Golgi DHHC proteins blocks SNAP25 palmitoylation (29, 32); (iii) palmitoylation of a CSP mutant trapped on ER membranes only occurs when ER and Golgi membranes are mixed by BFA treatment (16).

Several distinct mechanisms could account for newly synthesized SNAP25 and CSP (and other peripheral membrane proteins) being palmitoylated specifically at the Golgi: (i) DHHC proteins with specificity for these substrates are targeted exclusively to the Golgi, (ii) essential co-factors required for palmitoylation of these substrates are spatially restricted to the Golgi (*e.g.* the DHHC9 accessory protein GCP16 (33)), and/or (iii) the non-palmitoylated forms of these substrates have a high affinity for Golgi membranes. To explore these different possibilities, we added the ER localization signals from DHHC4, DHHC6 and UDP-glucuronyl transferase onto DHHC3, which was chosen due to its broad substrate specificity toward peripheral proteins (7, 16–19). All three ER retrieval signals promoted the complete relocation of DHHC3 onto ER membranes. We did not detect obvious association of the mutants with Golgi, TGN, or recycling endosome membranes as assessed by confocal microscopy. Despite this dramatic change in the localization of DHHC3 induced by the attached dilysine motifs, the mutant proteins displayed a similar ability as wild-type DHHC3 to palmitoylate SNAP25 and CSP. This observation is generally consistent with the notion that spatially restricted palmitoyla-

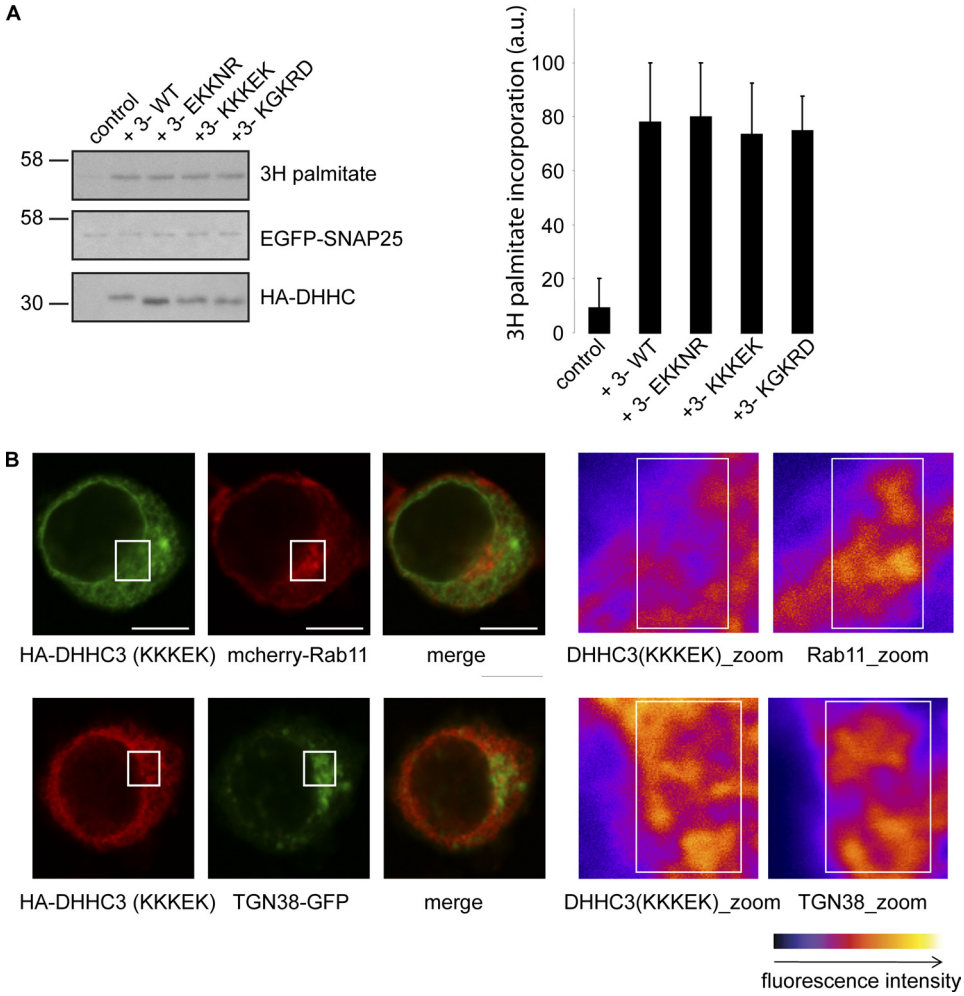

FIGURE 7. **Palmitoylation of SNAP25 by ER-localized DHHC3.** *A*, HEK293T cells were co-transfected with 0.8 μg of EGFP-SNAP25b and 1.6 μg of DHHC3 or the indicated mutants and analyzed ~20 h post-transfection. *Control* indicates EGFP-SNAP25b transfected with an empty vector (*i.e.* no DHHC co-expression) The transfected cells were labeled with [^{3}H]palmitic acid for 3 h, lysed in sample buffer, resolved by SDS-PAGE, and transferred to triplicate nitrocellulose membranes. The membranes were exposed to film with the aid of a Kodak Biomax Transcreen LE intensifier screen for detection of [^{3}H]palmitate incorporation (*top*) or were probed with anti-GFP (*middle*) or anti-HA (*bottom*) for detection of expression levels of EGFP-SNAP25 and the DHHC3 proteins, respectively. The positions of molecular weight markers are shown on the *left* of all *panels*. The amount of [^{3}H]palmitic acid incorporated into EGFP-SNAP25 in the presence of the various DHHC3 proteins was determined by densitometry ($n = 3$) and is shown in the *graph* on the *right*. *B*, the HA-DHHC3(KKKEK) mutant was transfected together with mcherry-Rab11 (*top*) or TGN38-GFP (*bottom*) into PC12 cells. HA-DHHC3(KKKEK) was detected using an anti-HA antibody followed by an anti-mouse secondary antibody conjugated to either Alexa Fluor 488 (*top*) or Alexa Fluor 543 (*bottom*). Representative images acquired using a Leica SP5 confocal microscope are shown. *Scale bars*, 5 μm. The *boxed regions* highlighted on the images in the *first* and *second columns* are shown at higher magnification in the *zoom images*. The *boxed regions* in the *zoom images* are added to aid visual analysis of fluorescence overlap of the co-transfected proteins. *Error bars*, S.E.

tion of SNAP25 and CSP at the Golgi occurs due to the specific targeting of their partner DHHC proteins to this compartment.

Previous work has shown that dilysine motifs can function either as retrieval or retention signals, dependent upon the identity of the surrounding amino acids (34). One concern was that the palmitoylation activity of DHHC3 mutants bearing dilysine motifs might have reflected a very small fraction of the proteins, undetectable by confocal imaging, that reached the Golgi before being retrieved by the COPI machinery. Thus, to further examine whether ER-localized DHHC3 is an active palmitoyltransferase, we studied palmitoylation of an ER-trapped CSP mutant (CSP(4CL)). Importantly, palmitoylation of this mutant was only significantly increased by ER-localized DHHC3 mutants and not by Golgi-localized wild-type DHHC3. This observation provides strong evidence that DHHC3 localized to ER membranes is an active palmitoyltransferase.

Although CSP and SNAP25 are palmitoylated by the same subset of DHHC proteins in co-expression studies, it is interesting to note that whereas palmitoylation and stable membrane binding of newly synthesized SNAP25 is markedly inhibited by BFA treatment, CSP is unaffected (16, 35). BFA disrupts Golgi integrity and results in formation of a mixed ER-Golgi compartment. This difference in BFA sensitivities occurs despite the proposal that both proteins initially access membranes via an intrinsic weak membrane affinity of their respective cysteine-rich domains (16, 21). Because Golgi DHHC proteins retain palmitoyltransferase activity following BFA treatment (16), this might imply that non-palmitoylated SNAP25 exhibits a higher affinity for intact Golgi membranes

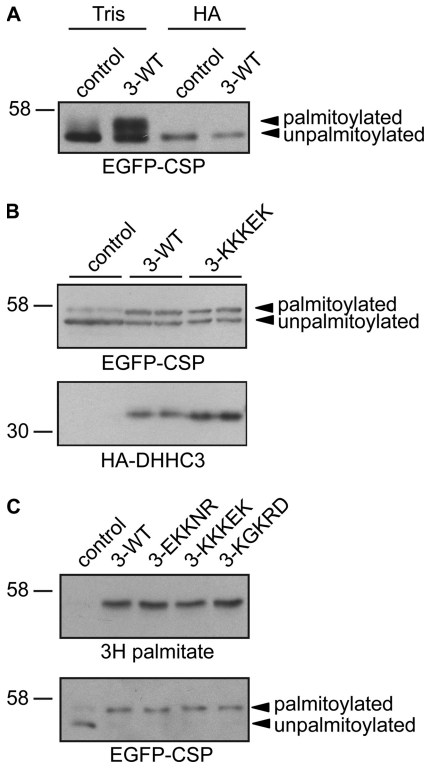

FIGURE 8. **Palmitoylation of CSP by ER-localized DHHC3.** *A*, 0.8 μg of EGFP-CSP was transfected into HEK293T cells with empty vector (*control*) or with 1.6 μg of HA-DHHC3 (*3-WT*). Twenty hours post-transfection, the cells were incubated either in 1 M Tris (pH 7) or 1 M hydroxylamine (pH 7) (*HA*) for 20 h at room temperature. The treated samples were then resolved by SDS-PAGE, transferred to nitrocellulose, and probed with an antibody against GFP. CSP undergoes a marked band shift following palmitoylation, and the positions of palmitoylated and unpalmitoylated CSP are highlighted by *arrowheads*. *B*, duplicate samples of cells transfected with EGFP-CSP alone (control) or with wild-type (*WT*) or ER-localized (*KKKEK*) DHHC3 were lysed 20 h post-transfection, resolved by SDS-PAGE, and transferred to nitrocellulose membrane for immunoblotting analysis using antibodies against the GFP or HA tags. *C*, cells co-transfected with EGFP-CSP and wild-type or ER-localized DHHC3 proteins were labeled with [^{3}H]palmitic acid for 3 h, lysed in sample buffer, resolved by SDS-PAGE, and transferred to duplicate nitrocellulose membranes. The membranes were exposed to film with the aid of a Kodak Biomax Transcreen LE intensifier screen for detection of [^{3}H]palmitate incorporation (*top*) or were probed with anti-GFP for detection of EGFP-CSP (*bottom*).

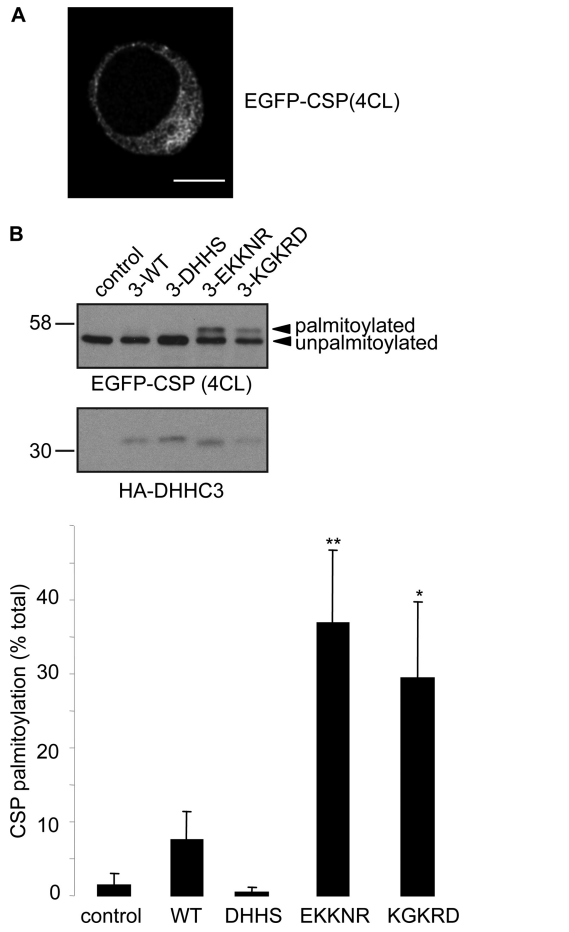

FIGURE 9. **Only ER-localized DHHC3 proteins are active against a CSP(4CL) mutant.** *A*, EGFP-CSP(4CL) mutant is localized to the ER. *Scale bar*, 5 μm. *B*, the CSP(4CL) mutant was co-transfected into HEK293 cells with wild-type or ER-localized DHHC3 mutants (*control* represents co-transfection with empty vector). The cells were lysed 20 h post-transfection, resolved by SDS-PAGE, and transferred to nitrocellulose membrane for immunoblotting analysis using antibodies against the GFP or HA tags. The CSP(4CL) mutant is not palmitoylated when expressed alone or together with wild-type DHHC3 (*WT*) or inactive DHHC3 (*DHHS*). In contrast, a band representing palmitoylated CSP(4CL) is apparent following co-transfection with ER-localized DHHC3 (EKKNR and KGKRD). The graph shows the percentage of CSP(4CL) palmitoylation following co-expression with the different DHHC3 proteins ($n = 3$). Only the ER-localized mutants (EKKNR and KGKRD) produced a significant increase in EGFP-CSP(4CL) palmitoylation compared with control (empty vector), analyzed using a one-way ANOVA (**, $p < 0.01$; *, $p < 0.05$). *Error bars*, S.E.

than for ER or fused ER-Golgi membranes. In this case, disruption of Golgi integrity by BFA would lead to an inhibition of SNAP25 palmitoylation because membrane interaction of the non-palmitoylated protein is reduced. Thus, a preference for interaction with Golgi membranes might also contribute (together with the specific targeting of partner DHHC proteins to the Golgi) to spatial patterning of SNAP25 palmitoylation. If this is the case, then overexpression of DHHC proteins at the ER may be sufficient to compensate for a lower affinity of the non-palmitoylated protein for ER *versus* Golgi membranes. It is clear, however, that many peripheral membrane proteins do not exhibit a strong preference for interaction with Golgi membranes in their non-palmitoylated state. As previously discussed, CSP palmitoylation and membrane binding is unaffected by BFA treatment (16), and thus for this protein, palmitoylation patterns are likely to be almost entirely directed by DHHC membrane targeting.

Interestingly, all three ER-localized DHHC3 proteins migrated at a lower molecular weight on SDS-polyacrylamide gels than wild-type DHHC3. This might suggest that DHHC3 undergoes a post-translational modification(s) upon delivery to the Golgi or the ER-Golgi intermediate compartment. At present, we do not know the nature of this modification, but glycosylation is a possibility. We do not believe that the different migration of wild-type and mutant forms of DHHC3 reflects differences in palmitoylation because the level of [^{3}H]palmitate labeling of the wild-type and mutant proteins was similar.

Many studies have highlighted DHHC3 as a highly active palmitoyltransferase with broad substrate specificity. In light of this, it was interesting that DHHC3 incorporated a greater amount of [^{3}H]palmitic acid than DHHC4 in the radiolabeling experiments reported herein. This difference does not imply that DHHC3 is more heavily palmitoylated than DHHC4, but it does point to palmitoylation of DHHC3 being more dynamic. Thus, perhaps a high intrinsic rate of palmitate turnover on

DHHC3 and the ease with which this enzyme "gives up" its attached palmitate groups to substrates is one reason why this DHHC protein is frequently identified as a highly active palmitoyltransferase. Nevertheless, DHHC4 has been suggested to be a functional palmitoyltransferase with activity toward β-secretase 1 (36).

At present, we do not know the importance of spatial restriction of palmitoylation of peripheral proteins, such as CSP and SNAP25, to the Golgi. One possibility is that palmitoylation-dependent trapping of these proteins at the Golgi is more conducive to the subsequent trafficking of the palmitoylated proteins to the plasma membrane. In this regard, it is interesting to note that vesicle budding from the Golgi was postulated to occur at cholesterol-rich membrane platforms (37). Because palmitoylated proteins have a high affinity for cholesterol-rich membranes (38), palmitoylation and subsequent lateral segregation of proteins at the Golgi may serve to provide a tight coupling between palmitoylation and plasma membrane delivery.

In summary, the work described provides an important step toward understanding how intracellular patterning of the DHHC family is achieved and clearly suggests that DHHC proteins are targeted in a manner to support spatially restricted and directed palmitoylation.

Acknowledgments—We are very grateful to Masaki Fukata for providing the HA-tagged DHHC constructs used in this study and to George Banting for the TGN38-GFP construct.

REFERENCES

1. Linder, M. E., and Deschenes, R. J. (2007) *Nat. Rev. Mol. Cell Biol.* **8,** 74–84
2. Fukata, Y., and Fukata, M. (2010) *Nat. Rev. Neurosci.* **11,** 161–175
3. Greaves, J., and Chamberlain, L. H. (2007) *J. Cell Biol.* **176,** 249–254
4. Salaun, C., Greaves, J., and Chamberlain, L. H. (2010) *J. Cell Biol.* **191,** 1229–1238
5. Lobo, S., Greentree, W. K., Linder, M. E., and Deschenes, R. J. (2002) *J. Biol. Chem.* **277,** 41268–41273
6. Roth, A. F., Feng, Y., Chen, L., and Davis, N. G. (2002) *J. Cell Biol.* **159,** 23–28
7. Fukata, M., Fukata, Y., Adesnik, H., Nicoll, R. A., and Bredt, D. S. (2004) *Neuron* **44,** 987–996
8. Greaves, J., and Chamberlain, L. H. (2011) *Trends Biochem. Sci.* **36,** 245–253
9. Hannoush, R. N., and Sun, J. (2010) *Nat. Chem. Biol.* **6,** 498–506
10. Kang, R., Wan, J., Arstikaitis, P., Takahashi, H., Huang, K., Bailey, A. O., Thompson, J. X., Roth, A. F., Drisdel, R. C., Mastro, R., Green, W. N., Yates, J. R., 3rd, Davis, N. G., and El-Husseini, A. (2008) *Nature* **456,** 904–909
11. Roth, A. F., Wan, J., Bailey, A. O., Sun, B., Kuchar, J. A., Green, W. N., Phinney, B. S., Yates, J. R., 3rd, and Davis, N. G. (2006) *Cell* **125,** 1003–1013
12. Rocks, O., Peyker, A., Kahms, M., Verveer, P. J., Koerner, C., Lumbierres, M., Kuhlmann, J., Waldmann, H., Wittinghofer, A., Bastiaens, P.I. (2005) *Science* **307,** 1746–1752
13. Goodwin, J. S., Drake, K. R., Rogers, C., Wright, L., Lippincott-Schwartz, J., Philips, M. R., and Kenworthy, A. K. (2005) *J. Cell Biol.* **170,** 261–272
14. Rocks, O., Gerauer, M., Vartak, N., Koch, S., Huang, Z. P., Pechlivanis, M., Kuhlmann, J., Brunsveld, L., Chandra, A., Ellinger, B., Waldmann, H., and Bastiaens, P. I. (2010) *Cell* **141,** 458–471
15. Bartels, D. J., Mitchell, D. A., Dong, X., and Deschenes, R. J. (1999) *Mol. Cell. Biol.* **19,** 6775–6787
16. Greaves, J., Salaun, C., Fukata, Y., Fukata, M., and Chamberlain, L. H. (2008) *J. Biol. Chem.* **283,** 25014–25026
17. Greaves, J., Gorleku, O. A., Salaun, C., and Chamberlain, L. H. (2010) *J. Biol. Chem.* **285,** 24629–24638.
18. Fernández-Hernando, C., Fukata, M., Bernatchez, P. N., Fukata, Y., Lin, M. I., Bredt, D. S., and Sessa, W. C. (2006) *J. Cell Biol.* **174,** 369–377
19. Fang, C., Deng, L., Keller, C. A., Fukata, M., Fukata, Y., Chen, G., and Lüscher, B. (2006) *J. Neurosci.* **26,** 12758–12768
20. Greaves, J., and Chamberlain, L. H. (2006) *Mol. Biol. Cell* **17,** 4748–4759
21. Greaves, J., Prescott, G. R., Fukata, Y., Fukata, M., Salaun, C., and Chamberlain, L. H. (2009) *Mol. Biol. Cell* **20,** 1845–1854
22. Greaves, J., and Chamberlain, L. H. (2011) *J. Cell Sci.* **124,** 1351–1360
23. Girotti, M., and Banting, G. (1996) *J. Cell Sci.* **109,** 2915–2926
24. Jackson, M. R., Nilsson, T., and Peterson, P. A. (1993) *J. Cell Biol.* **121,** 317–333
25. Rickman, C., Medine, C. N., Bergmann, A., and Duncan, R. R. (2007) *J. Biol. Chem.* **282,** 12097–12103
26. Palmer, Z. J., Duncan, R. R., Johnson, J. R., Lian, L. Y., Mello, L. V., Booth, D., Barclay, J. W., Graham, M. E., Burgoyne, R. D., Prior, I. A., and Morgan, A. (2008) *Biochem. J.* **413,** 479–491
27. Ohno, Y., Kihara, A., Sano, T., and Igarashi, Y. (2006) *Biochim. Biophys. Acta* **1761,** 474–483
28. Levy, A. D., Devignot, V., Fukata, Y., Fukata, M., Sobel, A., and Chauvin, S. (2011) *Mol. Biol. Cell* **22,** 1930–1942
29. Huang, K., Sanders, S., Singaraja, R., Orban, P., Cijsouw, T., Arstikaitis, P., Yanai, A., Hayden, M. R., and El-Husseini, A. (2009) *FASEB J.* **23,** 2605–2615
30. Greaves, J., Carmichael, J. A., and Chamberlain, L. H. (2011) *Mol. Biol. Cell* **22,** 1887–1895
31. Lemale, J., Bloch-Faure, M., Grimont, A., El Abida, B., Imbert-Teboul, M., and Crambert, G. (2008) *Biochim. Biophys. Acta* **1783,** 2234–2240
32. Singaraja, R. R., Huang, K., Sanders, S. S., Milnerwood, A. J., Hines, R., Lerch, J. P., Franciosi, S., Drisdel, R. C., Vaid, K., Young, F. B., Doty, C., Wan, J., Bissada, N., Henkelman, R. M., Green, W. N., Davis, N. G., Raymond, L. A., and Hayden, M. R. (2011) *Hum. Mol. Genet.* **20,** 3899–3909
33. Swarthout, J. T., Lobo, S., Farh, L., Croke, M. R., Greentree, W. K., Deschenes, R. J., and Linder, M. E. (2005) *J. Biol. Chem.* **280,** 31141–31148
34. Andersson, H., Kappeler, F., and Hauri, H. P. (1999) *J. Biol. Chem.* **274,** 15080–15084
35. Gonzalo, S., and Linder, M. E. (1998) *Mol. Biol. Cell* **9,** 585–597
36. Vetrivel, K. S., Meckler, X., Chen, Y., Nguyen, P. D., Seidah, N. G., Vassar, R., Wong, P. C., Fukata, M., Kounnas, M. Z., and Thinakaran, G. (2009) *J. Biol. Chem.* **284,** 3793–3803
37. Patterson, G. H., Hirschberg, K., Polishchuk, R. S., Gerlich, D., Phair, R. D., and Lippincott-Schwartz, J. (2008) *Cell* **133,** 1055–1067
38. Melkonian, K. A., Ostermeyer, A. G., Chen, J. Z., Roth, M. G., and Brown, D. A. (1999) *J. Biol. Chem.* **274,** 3910–3917